

## ANODIZATION AND OPTICAL APPEARANCE OF SPUTTER DEPOSITED Al-Zr COATINGS

Visweswara Chakravarthy Gudla<sup>1</sup>, Stela Canulescu<sup>2</sup>, Rajashekhara Shabadi<sup>3</sup>, Kristian Rechendorff<sup>4</sup>, Jørgen Schou<sup>2</sup>, Rajan Ambat<sup>1</sup>

<sup>1</sup>Department of Mechanical Engineering, Technical University of Denmark, DK-2800 Kgs. Lyngby, Denmark

<sup>2</sup>Department of Photonics Engineering, Technical University of Denmark, DK-4000 Roskilde, Denmark

<sup>3</sup>Unité Matériaux et Transformation (UMET) UMR CNRS 8207, Université Lille1, 59655 Villeneuve d'Ascq, France

<sup>4</sup>Tribology Centre, Danish Technological Institute, DK-8000 Århus C, Denmark

Keywords: Magnetron sputtering, Aluminium coating, Anodizing, Appearance

### Abstract

Anodized Al alloy components are extensively used in various applications like architectural, decorative and automobiles for corrosion protection and/or decorative optical appearance. However, tailoring the anodized layer for specific optical appearance is limited due to variation in composition and microstructure of the commercial alloys, and even more difficult with recycled alloys. Sputter coating methods promise to control the chemical composition of the Al alloy surfaces and eventually modify the microstructure of the surfaces with heat treatments thus enabling the freedom on the substrate quality. This paper evaluates the use of magnetron sputtered Al-Zr coatings on Al combined with heat treatment and anodizing for obtaining required optical properties. Metallurgical and optical characterization was carried out to investigate the effect of coating microstructure and anodizing parameters on appearance of the anodized layer. The microstructure of the coating is found to influence the appearance of anodized layer owing to the presence of completely or partially dissolved second phases during anodizing process. Oxidation status of the second phase particles in the coatings affected the light absorption and scattering phenomenon there by imparting different appearances to the anodized alloy surfaces.

### Introduction

Anodizing is widely applied to Al alloy components used in various industrial segments such as architecture for outdoor profiles, windows, facades, electronic consumer goods for decorative packaging and transportation for automobile components either for corrosion protection, optical appearance or both [1]. Of the several kinds of electrolytes used in anodizing of Al, sulphuric acid is the most commonly used for decorative anodizing [2]. The anodized layer for decorative applications is a transparent oxide layer whose appearance depends on the anodizing parameters and quality of the alloy surface being anodized [3,4]. Sulphuric acid anodizing gives in certain cases an anodized layer with self-assembled nano porous structure. This structure is impregnated with organic or inorganic dyes and later sealed, imparting different colours to the surface [2]. Optical appearance of the anodized layer is sometimes difficult [5] to control due to the increased use of recycled Al alloys because of the increased intermetallic phases in recycled Al alloys [6] which behave differently from the Al matrix during the anodizing process [1,7]. Many authors have reported the electrochemical behaviour of the second phases in various Al alloys during anodizing [8-11], on the other hand not much has been reported on the influence of second phase particles on the optical appearance after anodizing [12]. Recent studies show the potential use of sputtered coatings of binary and ternary alloy systems for understanding the anodizing behaviour of Al based phases [13].

Sputter coating techniques provide surfaces with a wide range of compositions which cannot be obtained by conventional melt and cast techniques. Once the coating composition, heat treatment and the anodizing processes are optimized, they can be deposited on any kind of Al alloy substrates, be it cast, wrought or recycled. By additional controlled heat treatments the microstructure could be varied to obtain desired second phase particles which upon anodizing are expected to modify the interaction of light in terms of scattering and absorption, and thus alter the optical appearance. The anodizing behaviour of several binary alloys systems like Al-Cu [14,15], Al-Mg [16], Al-Mn [17] and Al-Zn [18], prepared by sputter coating techniques, have been studied earlier in terms of morphology of anodized layer, migration of alloy species, adhesion and delamination of anodic films but their effect on optical appearance after anodizing is not reported. Another important class of materials based on Al-Zr alloys has not been addressed in the literature. A high refractive index of 2.2 for ZrO<sub>2</sub> [19] which is larger than that of anodized aluminium (n=1.7) [20,21] makes it an ideal candidate for optical effects. This difference in refractive index is expected to influence the optical appearance of the anodized surface. In order to understand and tailor the optical appearance of anodized surface, model Al-Zr alloy coatings on a pure aluminium surface with a varying concentration prepared by sputter coating technique is studied in detail. The effect of heat treatment and anodizing voltage along with composition, microstructure and morphology of second phases on the optical appearance of the anodized layer is discussed.

### Experimental

#### Materials and methods

Al substrates (Reinal™, 99.9 % purity) of dimensions 200 x 30 x 8 mm<sup>3</sup> were prepared from billets obtained from Alcan rolled products, Germany. The Al-Zr coatings with a composition gradient from 6 wt.% to 23 wt.% Zr were deposited using DC magnetron sputtering (Model CemeCon 800/8) at Tribology Centre, Danish Technological Institute, Denmark. The deposition was performed with a starting pressure of 4 mPa, and with a bias voltage of -50 V. One commercial AA1050 and another AA1050 target with Zr inserts were used in the sputtering chamber for obtaining the desired Zr concentration gradient during the coating process. The thickness of the coatings obtained was approximately 15 µm.

Heat treatment of the coated samples was performed in a muffle furnace at a temperature of 550 °C for 4 h. The samples were then removed from the furnace and cooled in ambient air. The heat treated and as received samples were then mechanically polished, buffed, and degreased in a mild Alifclean™ solution at 60 °C before being subjected to anodizing. The samples were then

subsequently de-smutted by immersing in diluted HNO<sub>3</sub> followed by rinsing with demineralised water. This process resulted in the removal of 5 - 6 μm of the coating thickness. Anodizing was carried out in a 20 wt.% sulphuric acid bath maintained at 18 °C; voltage used were 12.5 V and 20 V for different time periods aimed at achieving equal anodized layer thicknesses. This was followed by rinsing with demineralized water. Sealing of the anodized layer was performed in water at 96 °C for 25 min followed by drying with hot air.

### Spectrophotometry

Spectrally resolved optical reflectance of the coatings was measured using an integrating sphere-spectrophotometer setup. The samples were illuminated with a collimated beam from a deuterium tungsten-halogen light source (type DH2000 from Ocean Optics) at an angle of incidence of 8° with respect to normal. The reflected light was collected using an optical fibre coupled to an optical spectrometer (QE 65000 from Ocean Optics). Each reflectance spectrum was averaged over 4 s over the wavelength range from 350-750 nm. Diffuse reflectance of a sample was measured directly using a gloss trap coated with a dark absorbing material in the specular light port of the sphere. The specular reflectance spectrum is obtained by subtracting the diffuse reflectance from total reflectance of each sample. The spectrophotometer was calibrated using high specular and high diffuse reflectance standards.

### X-ray Diffraction

Grazing incidence X-ray diffraction (Model Bruker Discover D8) analysis was performed using Cu K<sub>α</sub> radiation at 40 kV and 40 mA for the phase analysis of as received and heat treated coatings before and after anodizing. The XRD patterns were recorded in the 2θ range from 10° to 100° with an incidence angle of 0.25°, step size of 0.01° and a scan step time of 3 s.

### Electron Microscopy

The morphology and microstructure of sputtered coatings after heat treatment and anodizing was observed using a scanning electron microscope (Model Quanta 200 ESEM FEG, FEI) equipped with an EDS (Oxford Instruments 80 mm<sup>2</sup> X-Max). The samples were mounted in an epoxy and polished to reveal the cross section. Transmission electron microscopy analysis was carried out on the sample cross section in the anodized as well as non-anodized regions using a TEM (Model Tecnai G2-20) operating at 200 keV. The lamellas for TEM were prepared using focused ion beam milling and insitu lift out in the microscope (Model Quanta 200 3D DualBeam, FEI) which was further thinned in a FIB-SEM (Model Helios Nanolab DualBeam, FEI).

## **Results**

### Visual Appearance

The optical appearance of the samples which were heat treated and anodized at 12.5 V and 20 V is shown in figure 1 for three surfaces with different Zr concentrations. Samples which are anodized at 20 V are brighter than those anodized at 12.5 V for all the Zr concentration range. Also, the appearance darkens with increasing Zr concentration.

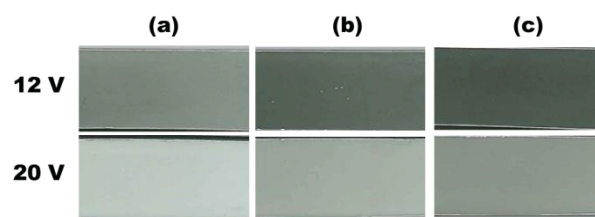


Figure 1: Optical images showing appearance of the anodized layer on Al-Zr coatings for Zr concentrations of (a) 9 wt.%, (b) 15 wt.% and (c) 21 wt.% after heat treatment and anodizing at different voltage.

### Spectrophotometry

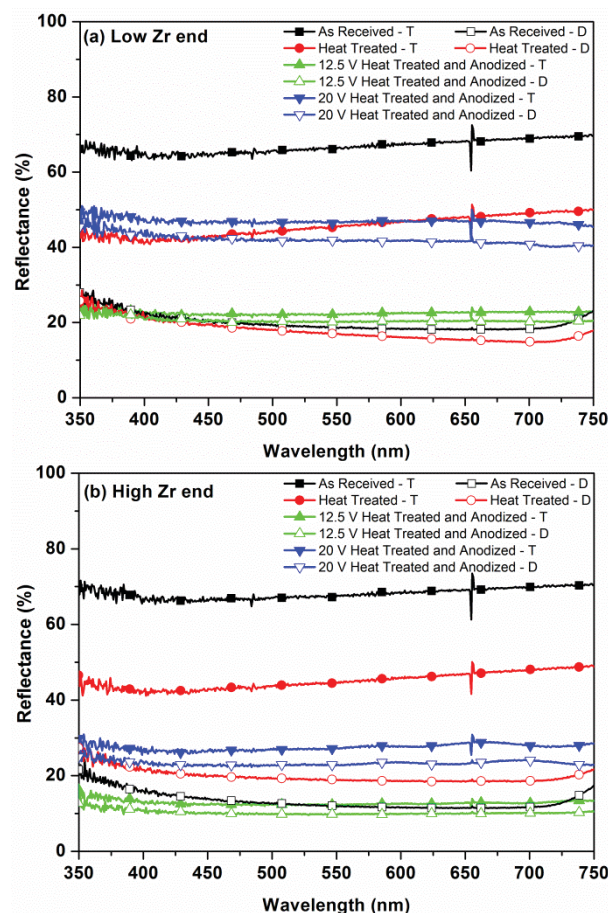


Figure 2: Reflectance spectra at visible wavelength region for Al-Zr coatings on pure Al in different conditions taken at location of (a) Low Zr content and (b) High Zr content; T-Total reflectance and D-Diffuse reflectance.

The diffuse and total reflectance spectra of the samples taken at a location corresponding to a Zr concentration of 9 wt.% (low Zr end) are shown in figure 2 (a). It can be seen that the as-received sample after polishing has a total reflectance and a diffuse reflectance value corresponding to approximately half of the total reflectance value. The specular reflectance is calculated as the difference between the total and diffuse reflectance. In the case of as received sample it can be seen that it is highly specular in nature, which is characteristic of a polished metal surface. After heat treatment, the total reflectance value reduces considerably and same is the case with the diffuse reflectance, however they are

also highly specular. Anodizing at 12.5 V after heat treatment reduces the total reflectance value to one third of the initial value for the as received and did not show significant difference between the diffuse and total reflectance value. On the other hand, the anodizing at 20 V results in a reflectance value that is higher compared to 12.5 V and the diffuse reflectance is as high as the total reflectance. The specular reflectance for the anodized samples is minimal implying that the samples lose their glossy nature and appear matte and diffuse. This pattern is observed across all the Zr concentration values in the sample. Spectra taken from sample positions corresponding to a Zr concentration of 21 wt.% (high Zr end) are presented for comparison purpose in figure 2 (b). The major difference observed when compared to spectra observed at high Zr is that the reflectance values are lower. This shows that the increase in Zr concentration makes the samples appear darker after anodizing, which is consistent with the results on visual appearance.

### X-Ray Diffraction

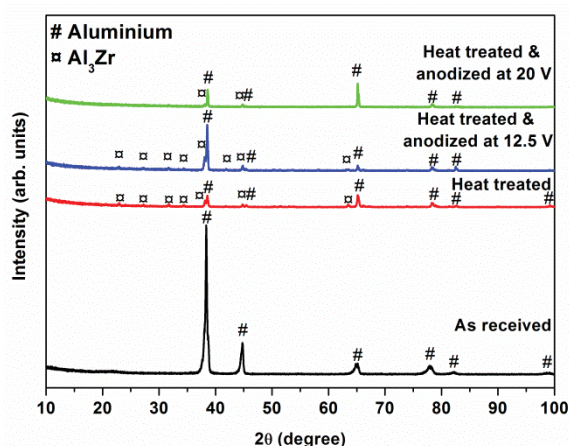


Figure 3: GI-XRD pattern for the as received, heat treated, and anodized samples at different voltages after heat treatment.

The GI-XRD pattern of the as-received, heat treated, and anodized samples are shown in figure 3. The diffraction pattern from the as-coated samples show peaks which correspond to the pure Al. There are no separate peaks which correspond to Zr or related phases, implying that all the Zr is dissolved in the Al matrix. The diffraction pattern of the heat treated samples shows peaks corresponding to Al and  $\text{Al}_3\text{Zr}$  phases. This is in accordance with the data obtained from the EDS results and the phase diagram for the Al-Zr binary system. The anodizing process does not give rise to any new sharp peaks in the pattern as it transforms the surface to an amorphous structure. The intensity of the peaks from  $\text{Al}_3\text{Zr}$  phase is lower in the case of samples anodized at 20 V when compared to those at 12.5 V. This might be due to the higher degree of transformation to amorphous phase of the sample when anodized at 20 V.

### Scanning Electron Microscopy

Figure 4 (a) shows the cross section of the anodized layer and the underlying coating after heat treatment in back scattered imaging mode. The coating after heat treatment shows uniform distribution of the precipitates with long baton type morphology throughout the thickness along with some irregular shaped precipitates in some regions. These precipitates principally appear in the

columnar structure arising out of the sputter deposition and growth process. The EDS data (not shown) of the long baton shaped second phases show the presence of Al and Zr, and the relative concentrations of the elements relates to  $\text{Al}_3\text{Zr}$  phase, which is expected according to the binary alloy Al-Zr phase diagram. Anodizing of the sputtered and heat treated coating at resulted in an anodized layer of approx. 2  $\mu\text{m}$  thickness (Fig. 4 (a), (b)), whereas the anodizing at 20 V resulted in slightly thinner anodized layer (Fig. 4 (c), (d)). It can be observed in anodized zone that, the baton shaped second phases are only partially transformed by the anodizing process at 12.5 V. The remaining non-anodized part of the precipitates appears to retain their contrast (shown with arrow) in the anodized coating (Fig. 4 (b)). The EDS analysis (not shown) of these non-anodized part does not show any appreciable changes in the concentrations of the constituting elements, but presence of little oxygen. The samples anodized at 20 V show more or less a complete transformation of the second phases to oxide as there is no contrast in the brightness on individual particles (Fig. 4 (d)). The structure and morphology of the coating was analysed for two other Zr concentrations and was observed to be similar.

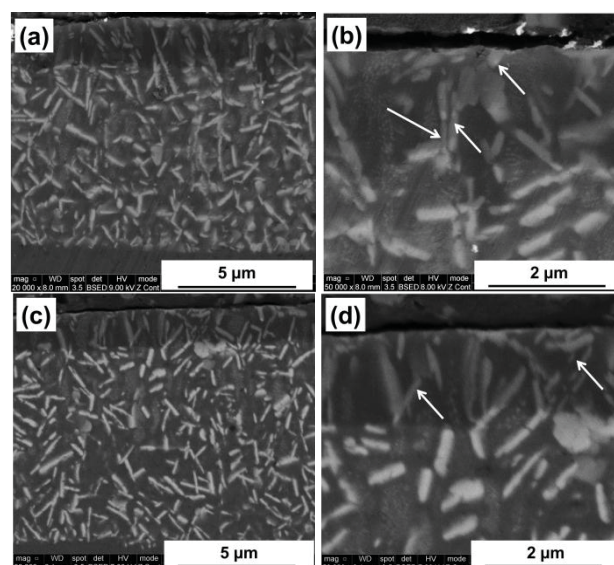


Figure 4. Back scattered electron images of Al-15 wt.% Zr coatings cross section on pure Al which were heat treated (550 °C for 4 h) and anodized at (a), (b) 12.5 V and (c), (d) 20 V in sulphuric acid.

### Transmission electron microscopy

Figure 5 (a) shows the bright field transmission electron micrograph in cross section of the sample heat treated and anodized at 12.5 V. The image shows the underlying heat treated sputtered coating containing big batons of  $\text{Al}_3\text{Zr}$  phases along with small precipitates. The anodizing process has completely transformed the matrix into oxide; while the precipitates are completely or partially transformed (presence of pore structure can be seen both in the matrix and precipitates). Two partially transformed precipitates can be observed in the pictures which are marked by arrows. High magnification image of the partially transformed precipitate marked in circle in figure 5 (a) is shown in figure 5 (b). The anodized region of the precipitate is transformed into amorphous phase as confirmed by the selective area diffraction analysis and the EDS data shows that it contains Al, Zr



and O (not shown), whereas the unaffected region is still crystalline.

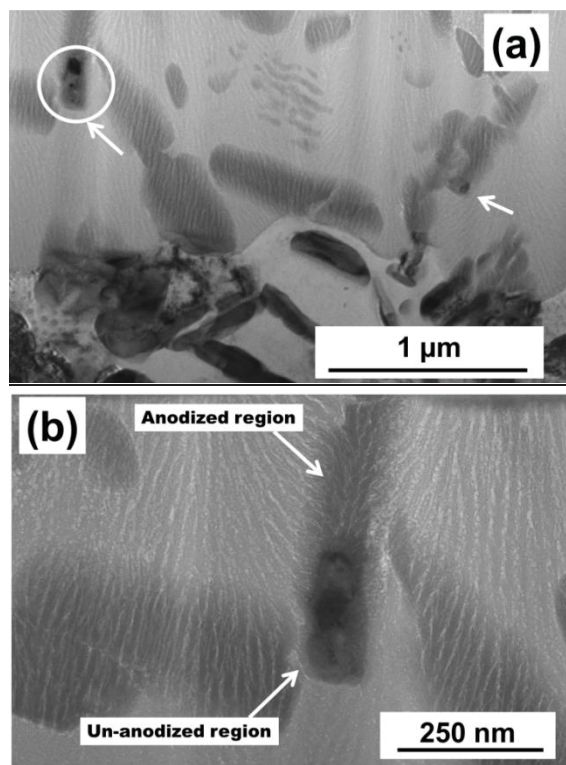


Figure 5: TEM bright field images of 12.5 V anodized sample showing: (a) anodized layer and underlying heat treated sputtered coating and (b) partially anodized  $\text{Al}_3\text{Zr}$  precipitate.

### Discussion

The SEM and XRD analysis show that sputter deposition process of Al-Zr targets gives a coating which has Zr dissolved in the Al matrix. The coatings are crystalline and columnar in nature. Heat treatment of these coatings results in uniform precipitation of  $\text{Al}_3\text{Zr}$  phase in a matrix of Al. Two types of precipitate morphology are detected in the heat treated coatings, one in the form of long batons and another fine precipitates. TEM analysis shows that the baton shaped precipitates and the Al matrix are transformed to amorphous oxides upon anodizing. The extent of transformation of the precipitates is dependent on their size and the voltage at which the anodizing is carried out. Lower anodizing voltages of 12.5 V only partially transform the precipitates whereas the anodizing at 20 V transform to a larger extent. The un-anodized region of the precipitates retains their crystalline and metallic nature whereas the oxidized part of the particles is essentially an amorphous mixture of oxides and hydroxides of Al and Zr.

As mentioned earlier, the difference in the refractive index between anodized Al and mixed oxide of Al-Zr is responsible for multiple scattering of light. The larger the number of particles that differ from the matrix in terms of refractive index, the larger the scattering of light. Homogenous distribution of such scattering centres in the anodized Al matrix results in the multiple scattering of light, which disperses the incident light in different directions and creates a diffuse appearance of the surface.

However, the un-anodized region of the  $\text{Al}_3\text{Zr}$  precipitates is still metallic and metals alloys have a high extinction coefficient, which is responsible for their absorption characteristics. The extinction coefficient becomes a prominent factor when the size range of the metal particles is comparable to the wavelength of visible light resulting in high absorption [22]. The current microstructure and morphology of the anodized layer is made up of multi-component metallic particles like  $\text{Al}_3\text{Zr}$  of various sub-micron sizes and shapes which serve as centres of absorption for the incoming light in an anodized Al surface and therefore induce a dark appearance of the heat treated and anodized samples.

The intensity or fraction of the light that is absorbed depends on the number of absorptive events taking place, which in turn is dependent on the number of metallic absorptive centres in the anodized Al matrix. At low Zr content, increasing the anodizing voltage from 12.5 V to 20 V results in fewer precipitates with metallic part in the anodized layer and hence the coatings appear brighter. The diffuse/total reflectance of the coatings increases by factor of two with increasing anodization voltage, and this is consistent with our observations across the Zr concentration range. At high Zr content, the fraction of un-anodized precipitates in the anodized layer for a given anodization voltage is much larger and is the reason for the darker appearance with increasing Zr content.

### Conclusions

Al-Zr coatings with Zr concentration varying from 6 wt.% to 23 wt.% on pure Al substrates are studied. The optical reflectivity of the anodized samples with heat treatment is found to be similar in response to wavelength throughout the Zr composition except that it is slightly darker with increasing concentration of Zr. Heat treatment of the coated samples results in  $\text{Al}_3\text{Zr}$  formation with a dual size distribution. Upon heat treatment, smaller sized second phases (<100 nm) and larger baton shaped precipitates are formed. Anodizing in sulphuric acid electrolyte at a voltage of 12.5 V, results in complete oxidation of small size second phase particles, while the larger particles are only partially oxidized. Upon increasing the anodizing voltage to 20 V, the extent of oxidation is increased. Amorphous oxides of Al and Zr serve as scattering centres in anodized Al matrix, but as they are only partially anodized they still act as absorption centres and lead to the dominantly absorbing behaviour of the specimen. Anodizing voltage of 20 V oxidizes the surface to a greater extent resulting in fewer absorption centres and hence the brighter appearance of the samples compared to those anodized at 12.5 V. From this study it is shown that the optical appearance of anodized Al alloys can be tailored to obtain a bright appearance by addition of alloying elements which upon anodizing would transform to oxides of high refractive index.

### Acknowledgements

The authors would like to thank the Danish National Advanced Technology Foundation for their financial support in the ODAAS project and all the involved project partners.

### References

- [1] S. Wernick, R. Pinner, P. G. Sheasby, and A. S. M. International., *The surface treatment and finishing of*

- aluminium and its alloys 1-2*. Teddington: Finishing Publ, 1987, pp. 1–47+1273 s. – 12 bd.
- [2] C. A. Grubbs, “Anodizing of aluminum,” *Met. Finish.*, vol. 105, no. 10, pp. 397–412, 2007.
- [3] F. Keller, M. Hunter, and D. Robinson, “Structural features of oxide coatings on aluminum,” *J. Electrochem. Soc.*, vol. 100, no. 9, pp. 411–419, 1953.
- [4] J. P. O’Sullivan and G. C. Wood, “The Morphology and Mechanism of Formation of Porous Anodic Films on Aluminium,” *Proc. R. Soc. A Math. Phys. Eng. Sci.*, vol. 317, no. 1531, pp. 511–543, Jul. 1970.
- [5] H. Zhu, T. Wei, M. J. Couper, and A. K. Dahle, “Effect of Fe-Rich Particles on the Formation of Die Streaks on Anodized Aluminum Extrusions,” *JOM*, vol. 64, no. 2, pp. 337–345, Feb. 2012.
- [6] G. Gaustad, E. Olivetti, and R. Kirchain, “Improving aluminum recycling: A survey of sorting and impurity removal technologies,” *Resour. Conserv. Recycl.*, vol. 58, no. 0, pp. 79–87, Jan. 2012.
- [7] M. Saenz de Miera, M. Curioni, P. Skeldon, and G. E. Thompson, “The behaviour of second phase particles during anodizing of aluminium alloys,” *Corros. Sci.*, vol. 52, no. 7, pp. 2489–2497, Jul. 2010.
- [8] H. Habazaki, K. Shimizu, P. Skeldon, G. E. Thompson, G. C. Wood, and X. Zhou, “Effects of alloying elements in anodizing of aluminium,” *Trans. Inst. Met. Finish.*, vol. 75, no. 1, pp. 18–23, 1997.
- [9] H. Habazaki, K. Shimizu, P. Skeldon, G. E. Thompson, G. C. Wood, and X. Zhou, “Nanoscale enrichments of substrate elements in the growth of thin oxide films,” *Corros. Sci.*, vol. 39, no. 4, pp. 731–737, 1997.
- [10] L. E. Fratila-Apachitei, H. Terryn, P. Skeldon, G. E. Thompson, J. Duszczyk, and L. Katgerman, “Influence of substrate microstructure on the growth of anodic oxide layers,” *Electrochim. Acta*, vol. 49, no. 7, pp. 1127–1140, Mar. 2004.
- [11] I. Tsangaraki-Kaplanoglou, S. Theohari, T. Dimogerontakis, Y.-M. Wang, H.H. (Harry) Kuo, and S. Kia, “Effect of alloy types on the anodizing process of aluminum,” *Surf. Coatings Technol.*, vol. 200, no. 8, pp. 2634–2641, Jan. 2006.
- [12] Y. Ma, X. Zhou, G. E. Thompson, J. O. Nilsson, M. Gustavsson, and A. Crispin, “Anodizing of AA6063 aluminium alloy profiles: Generation of dark appearance,” *Surf. Interface Anal.*, no. September 2012, Jan. 2013.
- [13] Y. Liu, M. A. Arenas, P. Skeldon, G. E. Thompson, P. Bailey, T. C. Q. Noakes, H. Habazaki, and K. Shimizu, “Anodic behaviour of a model second phase: Al–20at.%Mg–20at.%Cu,” *Corros. Sci.*, vol. 48, no. 5, pp. 1225–1248, May 2006.
- [14] H. H. Strehblow, C. M. Melliar Smith, and W. M. Augustyniak, “Examination of Aluminum Copper Films during the Galvanostatic Formation of Anodic Oxide: II. Rutherford Backscattering and Depth Profiling,” *J. Electrochem. Soc.*, vol. 125, no. 6, pp. 915–919, Jun. 1978.
- [15] H. Habazaki, X. Zhou, K. Shimizu, P. Skeldon, G. E. Thompson, and G. C. Wood, “Mobility of copper ions in anodic alumina films,” *Electrochim. Acta*, vol. 42, no. 17, pp. 2627–2635, 1997.
- [16] Y. Liu, P. Skeldon, G. E. Thompson, H. Habazaki, and K. Shimizu, “Anodic film growth on an Al–21at.%Mg alloy,” *Corros. Sci.*, vol. 44, no. 5, pp. 1133–1142, May 2002.
- [17] A. Crossland, G. E. Thompson, C. J. Smith, H. Habazaki, K. Shimizu, and P. Skeldon, “Formation of manganese-rich layers during anodizing of Al–Mn alloys,” *Corros. Sci.*, vol. 41, no. 10, pp. 2053–2069, Oct. 1999.
- [18] X. Zhou, H. Habazaki, K. Shimizu, P. Skeldon, G. E. Thompson, and G. C. Wood, “Enrichment-dependent anodic oxidation of Zinc in Al-Zn Alloys,” *Corros. Sci.*, vol. 38, no. 9, pp. 1563–1577, Sep. 1996.
- [19] R. A. Synowicki and T. E. Tiwald, “Optical properties of bulk c-ZrO<sub>2</sub>, c-MgO and a-As<sub>2</sub>S<sub>3</sub> determined by variable angle spectroscopic ellipsometry,” *Thin Solid Films*, vol. 455–456, no. 0, pp. 248–255, May 2004.
- [20] G. F. Pastore, “Transmission interference spectrometric determination of the thickness and refractive index of barrier films formed anodically on aluminum,” *Thin Solid Films*, vol. 123, no. 1, pp. 9–17, Jan. 1985.
- [21] I. H. Khan, J. S. L. Leach, and N. J. M. Wilkins, “The thickness and optical properties of films of anodic aluminium oxide,” *Corros. Sci.*, vol. 6, no. 11–12, pp. 483–497, 1966.
- [22] R. J. D. Tilley, “Colour due to Scattering,” in *Colour and the Optical Properties of Materials*, John Wiley & Sons, Ltd, 2010, pp. 175–196.